Available online at www.sciencedirect.com
ScienceDirect
International Journal of Heat and Fluid Flow 27 (2006) 937–944
International Journal of HEAT AND FLUID FLOW
www.elsevier.com/locate/ijhff

# Modelling turbulent collision rates of inertial particles

L.I. Zaichik [a,*], V.M. Alipchenkov [a], A.R. Avetissian [b]

[a] Institute for High Temperatures of the Russian Academy of Sciences, Krasnokazarmennaya 17a, 111116 Moscow, Russian Federation
[b] All Russian Nuclear Power Engineering, Research and Development Institute, Cosmonaut Volkov Str. 6a, 125171 Moscow, Russian Federation

Received 13 September 2005; received in revised form 28 January 2006; accepted 4 March 2006
Available online 15 June 2006

**Abstract**

The objective of the paper is to present a statistical model for predicting collision rates of inertial particles immersed in turbulent flow. This model is valid over the entire range of particle inertia (from the zero-inertia to the high-inertia limit) and accounts for two mechanisms influencing the collision rate, namely, the particle relative motion induced by turbulence and the accumulation effect that leads to an additional enhancement to the collision rate. The model is applicable to near-homogeneous two-phase turbulent flows with colliding or coalescing particles.


*Keywords:* Two-phase flow; Turbulence; Collision rate; Coalescence; Statistical model; Kinetic equation

## 1. Introduction

The rate of coagulation due to collisions of solid particles or liquid droplets in multiphase turbulent media is of importance in many environmental and industrial processes. Examples of turbulence-induced particle collisions include the formation of rain drops in clouds, precipitation of aerosols, agglomeration of fine powders in gas flows, pulverized coal combustion, dust and spray burners, pneumatic conveying, and so on. Because of the practical interest, a number of theoretical studies of the collision rate induced by turbulence have been performed. Relatively simple solutions to this problem may be derived with the assumption of homogeneous and isotropic turbulence. Two solutions are most familiar in the literature, corresponding to the limiting cases of zero-inertia and high-inertia particles. The first solution is valid for fine zero-inertia particles, whose collision rates are determined only by their interaction with small-scale energy-dissipating turbulent eddies (Saffman and Turner, 1956). The second solution relates to coarse high-inertia particles, whose motion is statistically independent and governed by the interaction with large-scale energy-containing turbulent eddies (Abrahamson, 1975). In both the zero-inertia and high-inertia limits, the particles are independently distributed with perfectly uniform probability, and hence the effect of preferential concentration is absent. However, of the most practical interest is the case of particles of intermediate inertia, when the ratios of the particle response time to the turbulence microscale and macroscale are finite. In this situation, it is necessary to take into consideration the interaction of particles with the overall spectrum of turbulent eddies as well as to account for the correlation of the motion of neighbouring particles and their preferential concentration.

The collision kernel is defined as the product of the half-surface of a collision sphere by both the mean radial relative velocity, $\langle|w_r|\rangle$, and the particle radial distribution function, $\Gamma$,

$$\beta = 2\pi d^2 \langle|w_r(d)|\rangle \Gamma(d). \tag{1}$$

It is clear from (1) that the turbulence-induced collision rate is governed by the mean relative velocity as well as by the radial distribution function. Consequently, the interaction of particles with turbulent eddies causes two statistical mechanisms that contribute to the collision rate: (i) the relative velocity between neighbouring particles (the so-called

* Corresponding author. Fax: +7 95 362 55 90.
*E-mail address:* leonid.zaichik@mtu-net.ru (L.I. Zaichik).

0142-727X/$ - see front matter © 2006 Elsevier Inc. All rights reserved.
doi:10.1016/j.ijheatfluidflow.2006.03.017

**Notation**

| | |
|---|---|
| $A_1$, $A_2$ | constants |
| $a$ | boundary condition parameter |
| $C$ | constant |
| $D^r_{\mathrm{p}\,ij}$ | particle-pair diffusivity tensor |
| $d$ | particle diameter |
| $\bar{d}$ | dimensionless particle diameter, $d/\eta$ |
| $f_r$, $g_r$, $f_{r1}$, $l_r$ | particle-pair response coefficients |
| $k$ | coalescence kernel |
| $N$ | number particle concentration |
| $P_w$ | two-point PDF |
| $p_w$ | two-point particle probability density |
| $\mathbf{R}_{\mathrm{p1}}$, $\mathbf{R}_{\mathrm{p2}}$ | particle positions |
| $\mathbf{r}$ | separation vector |
| $r$ | separation distance |
| $\mathbf{r}_{\mathrm{p}}$ | separation vector |
| $\bar{r}$ | dimensionless separation distance, $r/\eta$ |
| $Re_\lambda$ | Taylor-scale Reynolds number, $(15u'^4/\varepsilon\nu)^{1/2}$ |
| $S_{ij}$, $S_{\mathrm{p}\,ij}$ | second-order Eulerian fluid and particle velocity structure functions |
| $\bar{S}_{ij}, \bar{S}_{\mathrm{p}\,ij}$ | dimensionless fluid and particle structure functions, $S_{ij}/u_k^2$, $S_{p\ ij}/u_k^2$ |
| $S_{ijk}$,$S_{\mathrm{p}\,ijk}$ | third-order Eulerian fluid and particle velocity structure functions |
| $St$ | Stokes number |
| $\overline{T}_{\mathrm{L}}$ | dimensionless Lagrangian timescale of fluid turbulence |
| $T_{\mathrm{Lr}}$ | Lagrangian timescale of fluid velocity increment |
| $\overline{T}_{\mathrm{Lr}}$ | dimensionless Lagrangian timescale of fluid velocity increment, $T_{Lr}/\tau_k$ |
| $t$ | time |
| $U$ | mean axial velocity of the carrier fluid |
| $\mathbf{u}$ | fluid velocity |
| $u_{\mathrm{k}}$ | Kolmogorov velocity microscale, $(\nu\varepsilon)^{1/4}$ |
| $u'^2$ | fluid velocity variance |
| $\mathbf{v}_{\mathrm{p1}}$, $\mathbf{v}_{\mathrm{p2}}$ | particle velocities |
| $W_i, w_i, w'_i$ | mean, total and fluctuating relative velocities |
| $\mathbf{w}_{\mathrm{p}}$ | relative velocity between two particles |
| $\langle\lvert w_r\rvert\rangle$ | mean radial relative velocity between two particles |
| $x$ | distance from the channel inlet |

*Greeks*

| | |
|---|---|
| $\beta$ | collision kernel |
| $\Gamma$ | radial distribution function |
| $\Delta U_i, \Delta u'_i$ | mean and fluctuating fluid velocity increments |
| $\delta$ | delta-function or functional derivative |
| $\varepsilon$ | turbulent energy dissipation rate |
| $\eta$ | Kolmogorov length microscale, $(\nu^3/\varepsilon)^{1/4}$ |
| $\nu$ | fluid kinematic viscosity |
| $\rho$ | fluid density |
| $\rho_{\mathrm{p}}$ | particle density |
| $\tau$ | time increment |
| $\tau_{\mathrm{k}}$ | Kolmogorov time microscale, $(\nu/\varepsilon)^{1/2}$ |
| $\tau_{\mathrm{p}}$ | particle response time |
| $\Psi_{\mathrm{Lr}}$ | autocorrelation function of fluid velocity increment |

turbulent transport effect) and (ii) the non-uniform particle distribution (the accumulation effect). The accumulation effect is measured by the particle radial distribution function that is the probability of observing a particle pair normalized by the corresponding value in a uniform suspension. The accumulation effect manifests itself as a tendency of heavy particles to preferentially concentrate in regions of high strain-rate and avoid regions of high vorticity due to the centrifugal force. The investigations of Squires and Eaton (1991), Wang and Maxey (1993), Sundaram and Collins (1997), Balkovsky et al. (2001), Février et al. (2001), Hogan and Cuzzi (2001), Kostinski and Shaw (2001), Elperin et al. (2002), Sigurgeirsson and Stuart (2002), and Bec (2003) suggest that preferential particle concentration is mainly governed by small-scale dissipation-range turbulent structures, that is, clustering is most effective for particles whose response time matches with the Kolmogorov timescale of fluid turbulence. In Zaichik and Alipchenkov (2003), the accumulation phenomenon is treated as a result of a particle migration drift in the separation direction due to the gradient of the radial relative fluctuating velocity. This drift leads to the collection of particle pairs at small separations and hence acts in perfect analogy to an additional attractive force. Thus, the effect of preferential concentration is capable of making substantial increases in both collision and coagulation rates of inertial particles (Reade and Collins, 2000; Wang et al., 2000; Falkovich et al., 2002; Zaichik et al., 2003; Chun and Koch, 2005).

In this paper we present a statistical model for the collision rate of arbitrary-inertia particles dispersed by fluid turbulence. The paper extends the collision model given in Zaichik et al. (2003) to take properly account of the influence of particle size on two-particle velocity statistics and preferential concentration. Moreover, the model includes the transport effect in the approximations of Lagrangian velocity correlations.

## 2. Two-point PDF model

Let us first consider the two-point probability density function (PDF) model. This model is suitable for predicting two-particle statistics and particle-pair dispersion in homogeneous isotropic turbulence. The particle volume fraction is kept small enough so that the two-phase system is quite good within the dilute limit; therefore, only double colli-

sions between particles are taken into consideration. The density of particles is assumed to be much more than that of the carrier continuous phase (in this case, the drag force acting on a particle by the surrounding fluid flow is only of importance), and the particle size is small as compared to the Kolmogorov lengthscale.

Equations for two separate particles provide the equations describing the relative motion of a particle pair:

$$\frac{\mathrm{d}\mathbf{r}_\mathrm{p}}{\mathrm{d}t} = \mathbf{w}_\mathrm{p}, \quad \frac{\mathrm{d}\mathbf{w}_\mathrm{p}}{\mathrm{d}t} = \frac{\Delta\mathbf{u}(\mathbf{r}_\mathrm{p}, t) - \mathbf{w}_\mathrm{p}}{\tau_\mathrm{p}}. \tag{2}$$

Here $\mathbf{r}_\mathrm{p} \equiv \mathbf{R}_{\mathrm{p}2} - \mathbf{R}_{\mathrm{p}1}$ and $\mathbf{w}_\mathrm{p} \equiv \mathbf{v}_{\mathrm{p}2} - \mathbf{v}_{\mathrm{p}1}$ denote the separation distance and the relative velocity between two particles, whereas $\Delta\mathbf{u}(\mathbf{r}_\mathrm{p}, t) \equiv \mathbf{u}(\mathbf{R}_{\mathrm{p}2}, t) - \mathbf{u}(\mathbf{R}_{\mathrm{p}1}, t)$ is the increment in velocities at two points in which the particles are located. To proceed from stochastic Eq. (2) to the statistical description of the relative motion of two particles, the pair PDF is introduced:

$$P_w = \langle p_w \rangle = \langle \delta(\mathbf{r} - \mathbf{r}_\mathrm{p}(t)) \delta(\mathbf{w} - \mathbf{w}_\mathrm{p}(t)) \rangle. \tag{3}$$

The pair PDF, $P_w(\mathbf{r}, \mathbf{w}, t)$, describes the probability of finding a pair of particles separated by a distance $\mathbf{r}$, with a relative velocity $\mathbf{w}$, at time $t$. Differentiating (3) with respect to time and accounting for (2), we obtain a kinetic equation for the pair PDF:

$$\frac{\partial P_w}{\partial t} + w_k \frac{\partial P_w}{\partial r_k} + \frac{1}{\tau_\mathrm{p}} \frac{\partial (\Delta U_k - w_k) P_w}{\partial w_k} = -\frac{1}{\tau_\mathrm{p}} \frac{\partial \langle \Delta u'_k p_w \rangle}{\partial w_k}. \tag{4}$$

To determine the correlation $\langle \Delta u'_k p_w \rangle$ that quantifies eddy-particle interactions, the fluid relative velocity field is modelled by a Gaussian random process with known two-point correlation moments. Then, using the functional formalism and the Furutsu–Donsker–Novikov formula for Gaussian random functions, we can derive the following expression for the correlation between the fluid velocity increment and the particle-pair probability density (Zaichik and Alipchenkov, 2005):

$$\langle \Delta u'_i p_w \rangle = -S_{ij} \left( f_r \frac{\partial P_w}{\partial w_j} + \tau_\mathrm{p} g_r \frac{\partial P_w}{\partial r_j} \right) + \frac{\tau_\mathrm{p} f_{r1}}{2} \frac{DS_{ij}}{Dt} \frac{\partial P_w}{\partial w_j} - \tau_\mathrm{p} l_r S_{ik} \frac{\partial \Delta U_j}{\partial r_k} \frac{\partial P_w}{\partial w_j},$$

$$f_r = \frac{1}{\tau_\mathrm{p}} \int_0^\infty \Psi_\mathrm{Lr}(\tau) \exp\left(-\frac{\tau}{\tau_\mathrm{p}}\right) \mathrm{d}\tau, \quad g_r = \frac{T_\mathrm{Lr}}{\tau_\mathrm{p}} - f_r, \tag{5}$$

$$f_{r1} = \frac{1}{\tau_\mathrm{p}^2} \int_0^\infty \Psi_\mathrm{Lr}(\tau) \tau \exp\left(-\frac{\tau}{\tau_\mathrm{p}}\right) \mathrm{d}\tau, \quad l_r = g_r - f_{r1},$$

$$\frac{DS_{ij}}{Dt} = \frac{\partial S_{ij}}{\partial t} + \Delta U_k \frac{\partial S_{ik}}{\partial r_k} + \frac{\partial S_{ijk}}{\partial r_k}.$$

Here $S_{ij} \equiv \langle \Delta u'_i(\mathbf{r}) \Delta u'_j(\mathbf{r}) \rangle$ and $S_{ijk} \equiv \langle \Delta u'_i(\mathbf{r}) \Delta u'_j(\mathbf{r}) \Delta u'_k(\mathbf{r}) \rangle$ are the second-order and third-order fluid velocity structure functions. The coefficients $f_r$, $g_r$, $f_{r1}$, and $l_r$ measure a response of a pair of particles, separated by the distance $r$, to velocity fluctuations of the turbulent fluid, $\Psi_\mathrm{Lr}(\tau|r)$ symbolizes a Lagrangian autocorrelation function that describes the velocity increments of two fluid elements separated initially by the distance $r$, and $T_\mathrm{Lr} \equiv \int_0^\infty \Psi_\mathrm{Lr}(\tau)\mathrm{d}\tau$. When using the exponential approximation, $\Psi_\mathrm{Lr} = \exp(-\tau/T_\mathrm{Lr})$, the response coefficients become as follows:

$$f_r = \frac{T_\mathrm{Lr}}{\tau_\mathrm{p} + T_\mathrm{Lr}}, \quad g_r = \frac{T_\mathrm{Lr}^2}{\tau_\mathrm{p}(\tau_\mathrm{p} + T_\mathrm{Lr})},$$

$$f_{r1} = \frac{T_\mathrm{Lr}^2}{(\tau_\mathrm{p} + T_\mathrm{Lr})^2}, \quad l_r = \frac{T_\mathrm{Lr}^3}{\tau_\mathrm{p}(\tau_\mathrm{p} + T_\mathrm{Lr})^2}.$$

Substituting (5) into (4) yields the following kinetic equation for the two-point PDF of the particle-pair relative velocity distribution in homogeneous isotropic turbulence:

$$\frac{\partial P_w}{\partial t} + w_k \frac{\partial P_w}{\partial r_k} + \frac{1}{\tau_\mathrm{p}} \frac{\partial (\Delta U_k - w_k) P_w}{\partial w_k} + \frac{f_{r1}}{2} \frac{DS_{ik}}{Dt} \frac{\partial^2 P_w}{\partial w_i \partial w_k} = S_{ik} \left( \frac{f_r}{\tau_\mathrm{p}} \frac{\partial^2 P_w}{\partial w_i \partial w_k} + g_r \frac{\partial^2 P_w}{\partial r_i \partial w_k} + l_r \frac{\partial \Delta U_n}{\partial r_k} \frac{\partial^2 P_w}{\partial w_i \partial w_n} \right). \tag{6}$$

Eq. (6) describes the convective and diffusive transport in phase space $(\mathbf{r}, \mathbf{w})$ and resembles the one-point PDF equations (e.g., Derevich and Zaichik, 1988; Reeks, 1991; Simonin, 1996; Swailes and Darbyshire, 1997; Hyland et al., 1999; Pozorrski and Minier, 1999; Zaichik, 1999; Derevich, 2000; Pandya and Mashayek, 2003). However, the one-point and two-point kinetic equations bear a superficial resemblance, because the former deals with the one-particle PDF and hence does not take into consideration the spatial correlation of the motion of two particles. In contrast, the two-point statistical model allows for the spatial correlation between the velocities of particle pairs and thereby can predict the effect of clustering. The last term on the left-hand side part of (6) allows for the transport effect in the approximations of Lagrangian velocity correlations (Zaichik and Alipchenkov, 2005). When $DS_{ij}/Dt = \Delta\mathbf{U} = 0$, (6) reduces to the two-point PDF equation presented in Zaichik and Alipchenkov (2003).

Eq. (6) generates a set of balance equations governing the pair concentration, momentum, particulate stresses, or any appropriate statistical two-point moments of the relative velocity PDF. By this means the equations describing the particle-pair density, the mean relative velocity, and the second-order two-point structure function are written as:

$$\frac{\partial \Gamma}{\partial t} + \frac{\partial \Gamma W_k}{\partial r_k} = 0, \tag{7}$$

$$\frac{\partial W_i}{\partial t} + W_k \frac{\partial W_i}{\partial r_k} = -\frac{\partial S_{\mathrm{p}ik}}{\partial r_k} + \frac{\Delta U_i - W_i}{\tau_\mathrm{p}} - \frac{D^r_{\mathrm{p}ik}}{\tau_\mathrm{p}} \frac{\partial \ln \Gamma}{\partial r_k}, \tag{8}$$

$$\frac{\partial S_{\mathrm{p}ij}}{\partial t} + W_k \frac{\partial S_{\mathrm{p}ij}}{\partial r_k} + \frac{1}{\Gamma} \frac{\partial \Gamma S_{\mathrm{p}ijk}}{\partial r_k} + f_{r1} \frac{DS_{ij}}{Dt} = -(S_{\mathrm{p}ik} + g_r S_{ik}) \frac{\partial W_j}{\partial r_k} - (S_{\mathrm{p}jk} + g_r S_{jk}) \frac{\partial W_i}{\partial r_k} + l_r \left( S_{ik} \frac{\partial \Delta U_j}{\partial r_k} + S_{jk} \frac{\partial \Delta U_i}{\partial r_k} \right) + \frac{2}{\tau_\mathrm{p}} (f_r S_{ij} - S_{\mathrm{p}ij}), \tag{9}$$

where

$$\Gamma = \int P_w \mathrm{d}\mathbf{w}, \quad W_i = \frac{1}{\Gamma}\int w_i P_w \mathrm{d}\mathbf{w}, \quad S_{\mathrm{p}ij} = \langle w_i' w_j' \rangle = \frac{1}{\Gamma}\int (w_i - W_i)(w_j - W_j) P_w \mathrm{d}\mathbf{w},$$

$$S_{\mathrm{p}ijk} = \langle w_i' w_j' w_k' \rangle = \frac{1}{\Gamma}\int (w_i - W_i)(w_j - W_j)(w_k - W_k) P_w \mathrm{d}\mathbf{w},$$

$$D^r_{\mathrm{p}ij} = \tau_{\mathrm{p}}\left(S_{\mathrm{p}ij} + g_r S_{ij}\right).$$

To close the infinite equation set stemming from (6) at the second-order closure level of (7)–(9), we invoke a gradient algebraic approximation for the triple particle fluctuating velocity correlations. This approximation follows from the corresponding differential equation for the third moments by neglecting time evolution, convection, and generation due to mean velocity gradients as well as by using a quasi-Gaussian approximation for the fourth-rank correlations (Zaichik and Alipchenkov, 2003):

$$S_{\mathrm{p}ijk} = -\frac{1}{3}\left(D^r_{\mathrm{p}in}\frac{\partial S_{\mathrm{p}jk}}{\partial r_n} + D^r_{\mathrm{p}jn}\frac{\partial S_{\mathrm{p}ik}}{\partial r_n} + D^r_{\mathrm{p}kn}\frac{\partial S_{\mathrm{p}ij}}{\partial r_n}\right). \tag{10}$$

## 3. Particle dispersion in isotropic turbulence

In this section, the two-point PDF model is used for predicting pair dispersion in a steady-state suspension of particles immersed in homogeneous, isotropic, and stationary turbulence. In isotropic turbulence, due to spherical symmetry, the pair relative velocities and density distributions are independent of the orientation of the separation vector $\mathbf{r}$ and may be only dependent on $r \equiv |\mathbf{r}|$. Moreover, the mean convective transport in the fluid is supposed to be absent ($\Delta U_i = 0$), and the total number of particles is not changed in time. The latter infers that the balance between the net radial relative inward and outward fluxes takes place, and, therefore, the mean relative velocity, $W_i$, is equal to zero. By this means the set of Eqs. (7)–(9) along with (10) is constricted to the following system:

$$\frac{2\left(\overline{S}_{\mathrm{p}ll} - \overline{S}_{\mathrm{p}nn}\right)}{\bar{r}} + \frac{\mathrm{d}\overline{S}_{\mathrm{p}ll}}{\mathrm{d}\bar{r}} + \left(\overline{S}_{\mathrm{p}ll} + g_r\overline{S}_{ll}\right)\frac{\mathrm{d}\ln\Gamma}{\mathrm{d}\bar{r}} = 0, \tag{11}$$

$$\begin{aligned} St^2\Bigg\{&\frac{1}{\bar{r}^2\Gamma}\frac{\mathrm{d}}{\mathrm{d}\bar{r}}\left[\bar{r}^2\Gamma\left(\overline{S}_{\mathrm{p}ll} + g_r\overline{S}_{ll}\right)\frac{\mathrm{d}\overline{S}_{\mathrm{p}ll}}{\mathrm{d}\bar{r}}\right] - \frac{4}{3\bar{r}}\Bigg[\left(\overline{S}_{\mathrm{p}ll} + g_r\overline{S}_{ll}\right)\\ &\times\frac{\partial\overline{S}_{\mathrm{p}nn}}{\partial\bar{r}} + \frac{2}{\bar{r}}\left(\overline{S}_{\mathrm{p}nn} + g_r\overline{S}_{nn}\right)\left(\overline{S}_{\mathrm{p}ll} - \overline{S}_{\mathrm{p}nn}\right)\Bigg]\Bigg\}\\ &+ Stf_{r1}\Bigg\{\frac{1}{\bar{r}^2}\frac{\mathrm{d}}{\mathrm{d}\bar{r}}\left(\bar{r}^2\overline{T}_{\mathrm{Lr}}\overline{S}_{ll}\frac{\mathrm{d}\overline{S}_{ll}}{\mathrm{d}\bar{r}}\right)\\ &- \frac{4\overline{T}_{\mathrm{Lr}}}{3\bar{r}}\left[\overline{S}_{ll}\frac{\mathrm{d}\overline{S}_{nn}}{\mathrm{d}r} + \frac{2}{\bar{r}}\overline{S}_{nn}\left(\overline{S}_{ll} - \overline{S}_{nn}\right)\right]\Bigg\}\\ &+ 2\left(f_r\overline{S}_{ll} - \overline{S}_{\mathrm{p}ll}\right) = 0, \end{aligned} \tag{12}$$

$$\begin{aligned} &\frac{St^2}{3\bar{r}^4\Gamma}\Bigg\{\frac{\mathrm{d}}{\mathrm{d}\bar{r}}\left[\bar{r}^4\Gamma\left(\overline{S}_{\mathrm{p}ll} + g_r\overline{S}_{ll}\right)\frac{\mathrm{d}\overline{S}_{\mathrm{p}nn}}{\mathrm{d}\bar{r}}\right]\\ &\quad + 2\frac{\mathrm{d}}{\mathrm{d}\bar{r}}\left[\bar{r}^3\Gamma\left(\overline{S}_{\mathrm{p}nn} + g_r\overline{S}_{nn}\right)\left(\overline{S}_{\mathrm{p}ll} - \overline{S}_{\mathrm{p}nn}\right)\right]\Bigg\}\\ &\quad + \frac{Stf_{r1}}{3\bar{r}^4}\Bigg\{\frac{\mathrm{d}}{\mathrm{d}\bar{r}}\left(\bar{r}^4\overline{T}_{\mathrm{Lr}}\overline{S}_{ll}\frac{\mathrm{d}\overline{S}_{nn}}{\mathrm{d}\bar{r}}\right) + 2\frac{\mathrm{d}}{\mathrm{d}\bar{r}}\left[\bar{r}^3\overline{T}_{\mathrm{Lr}}\overline{S}_{nn}\left(\overline{S}_{ll} - \overline{S}_{nn}\right)\right]\Bigg\}\\ &\quad + 2\left(f_r\overline{S}_{nn} - \overline{S}_{\mathrm{p}nn}\right) = 0. \end{aligned} \tag{13}$$

Here and hereinafter the overbar stands for normalization by the Kolmogorov microscales, $St \equiv \tau_{\mathrm{p}}/\tau_k$ is the Stokes number that specifies the particle inertia, and $S_{\mathrm{p}ll}$ and $S_{\mathrm{p}nn}$ are the longitudinal and transverse components of the second-order particle velocity structure function $S_{\mathrm{p}ij}$.

Thus the model under consideration amounts to solving three non-linear ordinary differential equations involving the radial distribution function and the second-order longitudinal and transverse structure functions. Eq. (11) expresses the balance between the turbophoretic and diffusion forces in the separation direction between two particles.

Relevant boundary conditions for Eqs. (11)–(13) are given by:

$$\frac{\mathrm{d}\overline{S}_{\mathrm{p}ll}}{\mathrm{d}\bar{r}} = \frac{\mathrm{d}\overline{S}_{\mathrm{p}nn}}{\mathrm{d}\bar{r}} = 0 \quad \text{for } \bar{r} = a, \tag{14}$$

$$\overline{S}_{\mathrm{p}ll} = f_r\overline{S}_{ll}, \quad \overline{S}_{\mathrm{p}nn} = f_r\overline{S}_{nn}, \quad \Gamma = 1 \text{ for } \bar{r} \to \infty. \tag{15}$$

In (14), the case of $a = 0$ corresponds to elastic collisions of the so-called ghost (zero-size) particles, which are free to occupy any space in the suspension without being excluded by other particles (Reade and Collins, 2000; Zaichik and Alipchenkov, 2003). It seems likely that the approximation of ghost particles can provide prediction results, which are bound to be close to those obtained by Wang et al. (1998) and Wang et al. (2000) when using Scheme 1 for collision counting. In this collision-counting scheme, particles were allowed to overlap in the system and were not removed from the system after collision. The case of $a = \bar{d}$ appears to be appropriate for displaying the hard-sphere elastic collision model used by Sundaram and Collins (1997) and Reade and Collins (2000). Relations (15) point to the fact that the particle velocities become near-homogeneous at large separation, whereas the particles are randomly distributed.

The Eulerian longitudinal velocity structure function of the fluid is given by the approximation of Borgas and Yeung (2004):

$$\overline{S}_{ll} = \frac{2Re_\lambda}{15^{1/2}}\left[1 - \exp\left(-\frac{\bar{r}}{(15C)^{3/4}}\right)\right]^{4/3}\left(\frac{15^3\bar{r}^4}{15^3\bar{r}^4 + (2Re_\lambda/C)^6}\right)^{1/6}, \quad C = 2, \tag{16}$$

and the corresponding transverse structure function is expressed as:

$$\overline{S}_{nn} = \overline{S}_{ll} + \frac{\bar{r}}{2}\frac{\mathrm{d}\overline{S}_{ll}}{\mathrm{d}\bar{r}}.$$

The Lagrangian two-point timescale of velocity increment is approximated like (16) with the same constants as in Zaichik et al. (2003)

$$\overline{T}_{\mathrm{Lr}} = \overline{T}_{\mathrm{L}}\left[1-\exp\left(-\left(\frac{A_2}{A_1}\right)^{3/2}\bar{r}\right)\right]^{-2/3}\left(\frac{\bar{r}^4}{\bar{r}^4+(\overline{T}_{\mathrm{L}}/A_2)^6}\right)^{1/6},$$

$$A_1 = 5^{1/2}, \quad A_2 = 0.3.$$

Eqs. (11)–(13) along with boundary conditions (14) and (15) are solved numerically, and the results obtained are compared with DNS computations. In order to elucidate how the particle size affects pair dispersion and preferential concentration, we will also compare the prediction results obtained when using (14) with $a = 0$ and $a = \bar{d}$.

Fig. 1 demonstrates the ratio between the particle transverse and longitudinal structure functions for $\bar{r} = 1$ versus the Stokes number. For fluid elements as well as for zero-inertia particles, this ratio is two. In accordance with the DNS of Wang et al. (2000), the predicted ratio of $S_{\mathrm{p}\,nn}/S_{\mathrm{p}\,ll}$ that corresponds to zero-volume particles ($a = 0$) drops quickly and monotonically towards one as $St$ increases. The transverse-to-longitudinal structure function ratio predicted for finite-volume particles ($a = 1$) demonstrates a non-monotonic variation with Stokes number: $S_{\mathrm{p}\,nn}/S_{\mathrm{p}\,ll}$ decreases initially with $St$, reaching a minimum at $St \approx 2$, before increasing and finally approaching unity.

In Fig. 2 we compare the mean radial relative velocities predicted from (11)–(15) with those simulated by Wang et al. (2000). Under the assumption that the PDF of the relative velocity is Gaussian, the mean relative velocity magnitude is defined in terms of the longitudinal structure function as $\langle|\bar{w}_r|\rangle = (2\overline{S}_{\mathrm{p}\,ll}/\pi)^{1/2}$. Fig. 2 illustrates the influence of particle inertia on $\langle|\bar{w}_r|\rangle$ over a wide range of Stokes numbers. As is clear, the behaviour of $\langle|\bar{w}_r|\rangle$, with respect to $St$, is characterized by the presence of a maximum. The initial rise in $\langle|\bar{w}_r|\rangle$ is attributable to a decrease in the correlation of particle velocities with $\tau_{\mathrm{p}}$. The subsequent decay of $\langle|\bar{w}_r|\rangle$ beyond the maximum results from a decrease in the particle fluctuating velocities, since the particles become more sluggish and less responsive to the fluid turbulence. From Fig. 2, it is also seen that using $a = 0$ in boundary conditions (14) leads to slight smaller values of mean relative velocities at small $St$ as well as to better agreement with the DNS date as compared to the case of using $a = 1$. However, a difference in the mean relative velocities of zero-volume and finite-volume particles takes place only for relatively small Stokes numbers and vanishes at large $St$.

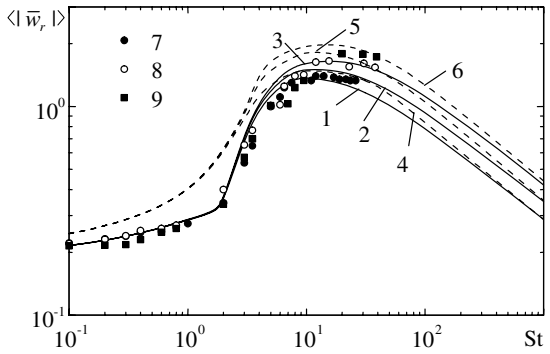


Fig. 2. Influence of particle inertia on the mean relative velocity magnitude for $\bar{r} = 1$: (1)–(3) – predictions with $a = 0$; (4)–(6) – predictions with $a = 1$; (7)–(9) – DNS by Wang et al. (2000); (1), (4), (7) – $Re_\lambda = 45$; (2), (5), (8) – $Re_\lambda = 58$; (3), (6), (9) – $Re_\lambda = 75$.

Fig. 3 demonstrates the radial distribution function for low-inertia zero-size and finite-size particles versus the separation distance between two particles. The radial distribution function for zero-size particles is singular when the separation equals to zero. It means that the accumulation (or clustering) effect of fine particles takes place. The accumulation phenomenon is treated as a result of a particle migration drift caused by the gradient of the radial relative fluctuating velocity. This drift leads to the collection of particle pairs at small separations and hence acts analogous to an additional attractive force. As is seen, the radial distribution function for finite-size particles deviates down from that for zero-size particles in the vicinity of the particle

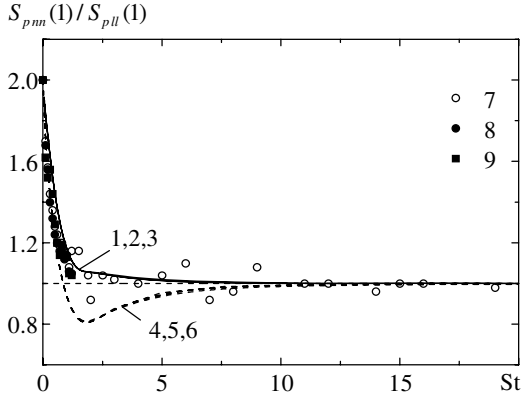


Fig. 1. Transverse-to-longitudinal structure function ratio for $\bar{r} = 1$: (1)–(3) – predictions for ghost particles ($a = 0$); (4)–(6) – predictions for finite-volume particles ($a = 1$); (7)–(9) – DNS by Wang et al. (2000); (1), (4), (7) – $Re_\lambda = 24$; (2), (5), (8) – $Re_\lambda = 45$; (3), (6), (9) – $Re_\lambda = 75$.

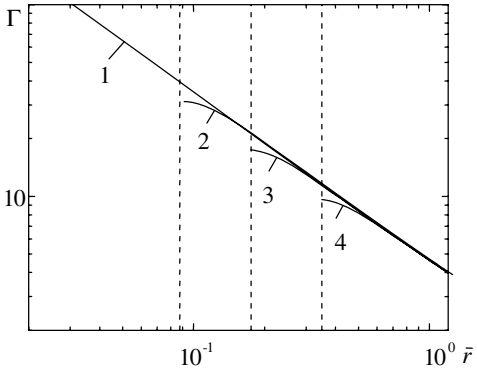


Fig. 3. The radial distribution function against the separation distance between two particles for $St = 1$ and $Re_\lambda = 54$: (1) – zero-volume particles ($a = 0$); (2)–(4) – finite-volume particles of size $a = 0.0875$, 0.175, and 0.35.

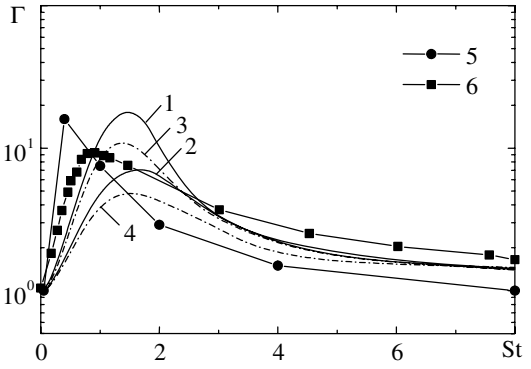


Fig. 4. Influence of particle inertia on the radial distribution function: (1)–(4) – predictions; (1), (2) – $a = 0$; (3) – $a = 0.36$; (4) – $a = 1$; (5) – DNS by Sundaram and Collins (1997); (6) – DNS by Wang et al. (2000); (1), (3), (5) – $\bar{r} = 0.36$, $Re_\lambda = 54$; (2), (4), (6) – $\bar{r} = 1$, $Re_\lambda = 58$.

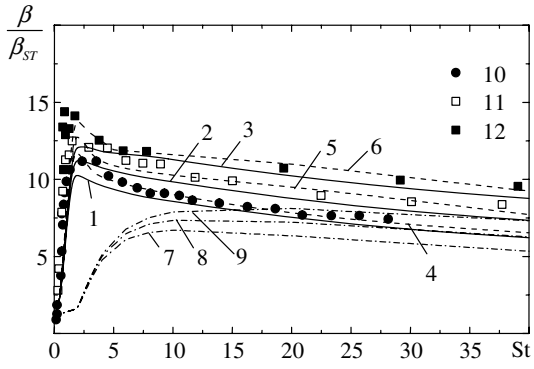


Fig. 5. Influence of particle inertia on the collision kernel for $\bar{d} = 1$: (1)–(3) – predictions with $a = 0$; (4)–(6) – predictions with $a = 1$; (7)–(9) – predictions with neglecting the accumulation effect; (10)–(12) – DNS by Wang et al. (2000); (1), (4), (7), (10) – $Re_\lambda = 45$; (2), (5), (8), (11) – $Re_\lambda = 58$; (3), (6), (9), (12) – $Re_\lambda = 75$.

diameter. Thus, the preferential concentration decreases with increasing particle size.

Fig. 4 shows the influence of particle inertia on the radial distribution function for separations and Reynolds numbers, which correspond to the DNS data of Sundaram and Collins (1997) and Wang et al. (2000). As expected, in the limiting cases of zero-inertia and high-inertia particles, the concentration field is statistically uniform, and therefore the radial distribution function is equal to unity. In accord with the computations, the predicted radial distribution function goes through a peak as the particle inertia time increases. Thus, there exists a critical particle response time which results in maximum preferential concentration. The value of this critical response time is of the same order as the Kolmogorov timescale, that is, the clustering is more considerable when tuning the particle parameters to the flow Kolmogorov scales. Fig. 4 demonstrates a qualitative agreement between the predicted and simulated particle distributions, although the predicted maxima of $\Gamma$ are slightly shifted towards particles with larger inertia. Fig. 4 also exhibits that the effect of finite particle size results in decreasing preferential concentration.

Finally let us consider the effect of particle inertia on the collision rate that is derived from the relationship:

$$\beta = \left(8\pi S_{p\,ll}(d)\right)^{1/2} d^2 \Gamma(d). \tag{17}$$

Fig. 5 represents the collision kernel normalized with the Saffman–Turner one for fine zero-inertia particles and compares predictions with the DNS data of Wang et al. (2000). As is seen, the model being developed properly captures the crucial trends of the DNS results, although the predicted maxima of $\beta$, much like $\Gamma$ in Fig. 4, are slightly shifted towards particles with larger inertia. The collision kernels, predicted when using $a = 1$ in boundary conditions (14), are slightly greater in values and better correspond to the DNS than those obtained for zero-size particles. It is also important to emphasise that the neglect of the accumulation effect leads to considerably less values of the collision rates of low-inertia particles than those given by DNS.

## 4. Particle agglomeration due to coalescence

One of the major motivations for developing the collision model described in the preceding sections is the simulation of the particle size evolution due to coalescence in aerosol reactors. Therefore, as an example of engineering application, we employ the collision model to evaluate the coalescing droplet size in a turbulent channel flow. We restrict the consideration to the channel core where the nearly homogeneous and isotropic flow conditions allow the application of the collision model developed. The particles are regarded as a mono-size suspension, and, consequently, the droplet size growth is treated as a sequence of the formation of doublets due to the loss of singlets (e.g., see Brunk et al., 1998). This simple coalescence model gives a rather crude approximation to the real agglomeration process and it may be solely used for estimating the droplet mean size. In such an interpretation of the agglomeration process, the depletion of the number particle concentration (number of particles per unit volume) along the channel axis is governed by the equation:

$$U\frac{\mathrm{d}N}{\mathrm{d}x} = -\frac{kN^2}{2}. \tag{18}$$

The coalescence kernel incorporates both the kinematic collision rate caused by fluid turbulence and the effect of interparticle interactions (e.g., van der Waals attraction and hydrodynamics) which are responsible for the collision efficiency. In what follows, the collision efficiency is assumed as unity, and hence the coalescence kernel, $k$, is inferred to be equal to the collision one, $\beta$. Moreover, because coalescence does not result in a change of the volume fraction, the following equation relating the number droplet concentration to the particle diameter takes place:

$$Nd^3 = N_0 d_0^3, \tag{19}$$

where the subscript 0 denotes the inlet values.

Let us consider the agglomeration process of droplets in the flow conditions, which correspond to DNS performed

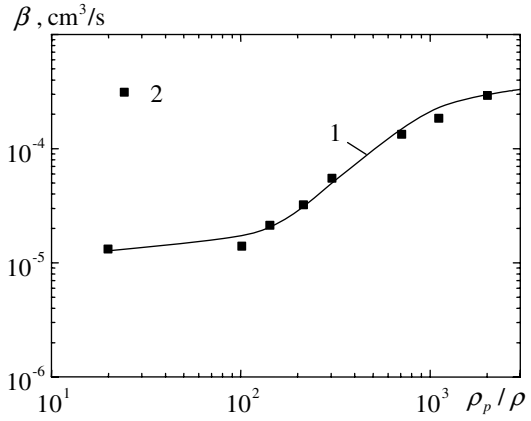


Fig. 6. Effect of the droplet-to-fluid density ratio on the collision kernel ($d = 9.96$ μm): (1) – model prediction, (2) – DNS by Chen et al. (1998).

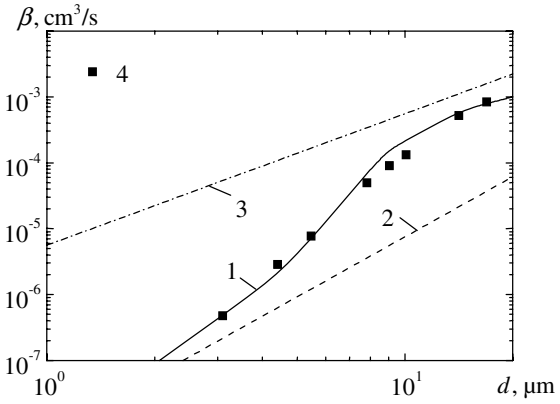


Fig. 7. Dependence of the collision kernel on the droplet diameter ($\rho_p/\rho = 713$): (1) – present model, (2) – Saffman and Turner (1956), (3) – Abrahamson (1975), (4) – DNS by Chen et al. (1998).

by Chen et al. (1998). In these simulations, the Reynolds number, $Re_\lambda$, at the channel centreline based on the Taylor length microscale and the turbulence intensity, averaged over the three coordinate directions, was 29.7. Figs. 6 and 7 show the performance of Eq. (17) for the prediction of the collision rate at the channel core. As is seen, both the droplet-to-fluid density ratio and the droplet diameter significantly influence the collision kernel. They affect the collision kernel because $\rho_p/\rho$ and $d$ affect the droplet inertia increasing the particle response time, $\tau_p$. When the density ratio decreases, the particle response time decreases as well and, according to Saffman and Turner (1956), $\beta$ becomes independent of $\rho_p/\rho$. For comparison, the results calculated from the Saffman–Turner and Abrahamson theories are also plotted in Fig. 7. It is clear that the Saffman–Turner collision rates, which do not take into account the droplet inertia, underestimate the DNS results and approach those only for the smallest droplets. Conversely, the Abrahamson theory, which does not take into consideration the velocity correlation between two colliding droplets, overestimates the DNS date. The collision rates based on the present model are in good agreement with the direct simulations. Thus, we can draw the conclusion that the model advanced for interparticle collisions in homogeneous isotropic turbulence may be successfully applied to predict particle coalescence in turbulent channel flow.

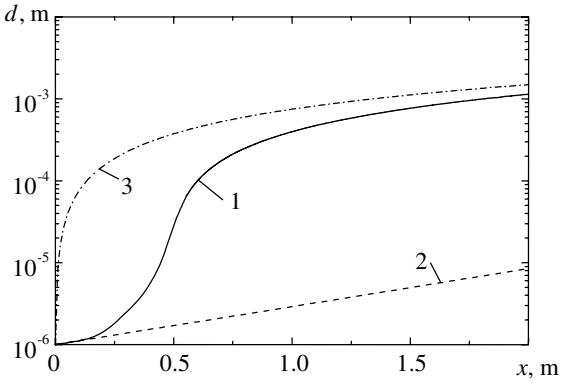


Fig. 8. Variation in the droplet size along the channel centerline: (1) – present collision model, (2) – Saffman–Turner theory, (3) – Abrahamson theory.

Fig. 8 displays variations in the droplet mean size along the channel core, which are obtained from Eq. (18) along with (19) for $d_0 = 1$ μm. Three different curves denote results based on the collision rates given by Eq. (17), Saffman and Turner (1956) and Abrahamson (1975), respectively. As one might expect, the Saffman–Turner and Abrahamson collision theories predict reasonable sizes of coalescing particles only in the limiting cases of small and large particles.

## 5. Summary

A statistical model for predicting the collision rate of inertial particles in homogeneous isotropic turbulence was developed. This model is based on a kinetic equation for the two-point PDF of the particle-pair relative velocity distribution. It accounts for two mechanisms influencing the collision rate: (i) the particle relative motion induced by turbulence and (ii) the preferential concentration that leads to an additional enhancement to the collision kernel. The model presented is valid over the entire range of Stokes numbers (from the zero-inertia to the high-inertia limit).

The effect of particle size on the relative fluctuating velocity, the radial distribution function, and the collision rate is investigated. A comparison between predictions obtained for zero-volume (ghost) and finite-volume particles is performed.

On the basis of comparisons with DNS results, it is concluded that the model presented is able to capture the main features of the collision rate of inertial particles in homogeneous isotropic and near-axis channel turbulent flows. This collision model appears to be applicable to the evaluation of the turbulence-induced agglomeration process in aerosol reactors.

## References


Abrahamson, J., 1975. Collision rates of small particles in a vigorously turbulent fluid. Chem. Eng. Sci. 30 (11), 1371–1379.

Balkovsky, E., Falkovich, G., Fouxon, A., 2001. Intermittent distribution of inertial particles in turbulent flows. Phys. Rev. Lett. 86 (13), 2790–2793.

Bec, J., 2003. Fractal clustering of inertial particles in random flows. Phys. Fluids 15 (11), L81–L84.

Borgas, M.S., Yeung, P.K., 2004. Relative dispersion in isotropic turbulence. Part 2. A new stochastic model with Reynolds-number dependence. J. Fluid Mech. 503, 125–160.

Brunk, B.K., Koch, D.L., Lion, L.D., 1998. Observations of coagulation in isotropic turbulence. J. Fluid Mech. 371, 81–107.

Chen, M., Kontomaris, K., McLaughlin, J.B., 1998. Direct numerical simulation of droplet collisions in a turbulent channel flow. II. Collision rates. Int. J. Multiphase Flow 24, 1105–1138.

Chun, J., Koch, D.L., 2005. Coagulation of monodisperse aerosol particles by isotropic turbulence. Phys. Fluids 17 (2), 027102-1–027102-15.

Derevich, I.V., 2000. Statistical modelling of mass transfer in turbulent two-phase dispersed flows. 1. Model development. Int. J. Heat Mass Transfer 43 (19), 3709–3723.

Derevich, I.V., Zaichik, L.I., 1988. Particle deposition from a turbulent flow. Fluid Dyn. 23 (5), 722–729.

Elperin, T., Kleeorin, N., L'vov, V.S., Rogachevskii, I., Sokoloff, D., 2002. Clustering instability of the spatial distribution of inertial particles in turbulent flows. Phys. Rev. E 66 (036302), 1–16.

Falkovich, G., Fouxon, A., Stepanov, M.G., 2002. Acceleration of rain initiation by cloud turbulence. Nature 419, 151–154.

Février, P., Simonin, O., Legendre, D., 2001. Particle dispersion and preferential concentration dependence on turbulent Reynolds number from direct and large-eddy simulations of isotropic homogeneous turbulence. In: Proc. of the Fourth International Conference on Multiphase Flow. New Orleans, pp. 1–8.

Hogan, R.C., Cuzzi, J.N., 2001. Stokes and Reynolds number dependence of preferential particle concentration in simulated three-dimensional turbulence. Phys. Fluids 13 (10), 2938–2945.

Hyland, K.E., McKee, S., Reeks, M.W., 1999. Deviation of a pdf kinetic equation for the transport of particles in turbulent flows. J. Phys. A: Math. Gen. 32, 6169–6190.

Kostinski, A.B., Shaw, R.A., 2001. Scale-dependent droplet clustering in turbulent clouds. J. Fluid Mech. 434, 389–398.

Pandya, R.V.R., Mashayek, F., 2003. Non-isothermal dispersed phase of particles in turbulent flow. J. Fluid Mech. 475, 205–245.

Pozorrski, J., Minier, J.-P., 1999. Probability density function modeling of dispersed two-phase turbulent flows. Phys. Rev. E 59 (1), 855–863.

Reade, W.C., Collins, L.R., 2000. Effect of preferential concentration on turbulent collision rates. Phys. Fluids 12 (10), 2530–2540.

Reeks, M.W., 1991. On a kinetic equation for the transport of particles in turbulent flows. Phys. Fluids A 3 (3), 446–456.

Saffman, P.G., Turner, J.S., 1956. On the collision of drops in turbulent clouds. J. Fluid Mech. 1 (1), 16–30.

Sigurgeirsson, H., Stuart, A.M., 2002. A model for preferential concentration. Phys. Fluids 14 (12), 4352–4361.

Simonin, O., 1996. Combustion in two-phase flows: Continuum modelling of dispersed two-phase flowsLecture Series 1996–2002. Von Karman Institute for Fluid Dynamics.

Squires, K.D., Eaton, J.K., 1991. Preferential concentration of particles by turbulence. Phys. Fluids A 3 (5), 1169–1178.

Sundaram, S., Collins, L.R., 1997. Collision statistics in an isotropic particle-laden turbulent suspension. Part 1. Direct numerical simulations. J. Fluid Mech. 335, 75–109.

Swailes, D.C., Darbyshire, K.F.F., 1997. A generalized Fokker–Plank equation for particle transport in random media. Physica A 242, 38–48.

Wang, L.-P., Maxey, R.M., 1993. Settling velocity and concentration distribution of heavy particles in homogeneous isotropic turbulence. J. Fluid Mech. 256, 27–68.

Wang, L.-P., Wexler, A.S., Zhou, Y., 1998. On the collision rate of small particles in isotropic turbulence. I. Zero-inertia case. Phys. Fluids 10 (1), 266–276.

Wang, L.-P., Wexler, A.S., Zhou, Y., 2000. Statistical mechanical description and modeling of turbulent collision of inertial particles. J. Fluid Mech. 415, 117–153.

Zaichik, L.I., 1999. A statistical model of particle transport and heat transfer in turbulent shear flows. Phys. Fluids 11 (6), 1521–1534.

Zaichik, L.I., Alipchenkov, V.M., 2003. Pair dispersion and preferential concentration of particles in isotropic turbulence. Phys. Fluids 15 (6), 1776–1787.

Zaichik, L.I., Alipchenkov, V.M., 2005. Statistical models for predicting particle dispersion and preferential concentration in turbulent flows. Int. J. Heat Fluid Flow 26, 416–430.

Zaichik, L.I., Simonin, O., Alipchenkov, V.M., 2003. Two statistical models for predicting collision rates of inertial particles in homogeneous isotropic turbulence. Phys. Fluids 15 (10), 2995–3005.